Nanotechnology Perceptions
ISSN 1660-6795
www.nano-ntp.com

Synthesis Of Cuo By Ctab-Assisted Hydrothermal Method

Anil Kumar Bedwal, Vikram Singh*

Research Scholar, OM Sterling Global University, Hisar, Email id: Anilkumarbedwal9@gmail.com
Assistant Professor, OM Sterling Global University, Hisar, Email id: Vikramdobal@gmail.com
Corresponding Author: Vikram Singh., Assistant Professor, OM Sterling Global University, Hisar, Email id: Vikramdobal@gmail.com*

A simple and cost-effective hydrothermal method was used to fabricate CuO thin films with nanostructures. The cetyltrimethyl ammonium bromide (CTAB) capping agent has been used to limit the development of copper oxide due to its water solubility and the metal-bonding capabilities of its ligands. Here, we skipped CTAB at a constant dosage and examined the effects of varying quantities of precursor copper sulfate on supercapacitance performance. The designed nanostructured materials were studied using state-of-the-art characterisation techniques as XRD, SEM, Cyclic Voltammetry, Charge Discharge, and others. Deposited CuO nanocrystalline thin films' specific capacitances, energy densities, and power densities were measured using the charge-discharge measuring technique.

Key words: CuO; nanostructures; magnification; CTAB; hydrothermal method.

INTRODUCTION

Hydrothermal processing changes several fundamental properties of water that impact its solvent capabilities by increasing its temperature and pressure, including its ionic product, density, thermal conductivity, viscosity, heat capacity, and dielectric constant. The synthesis parameters may be fine-tuned to provide solvent-specific properties, and these properties are pH-dependent. Since the dielectric constant decreases with increasing temperature, ionic species of solute may precipitate into a solid phase. Particles go through the nucleation process. The building blocks of nanostructures are the nucleation sites. Basic salt solutions, like metal chlorides, sulfates, or acetates, are often used as a starting point in the synthesis of inorganic nanoparticles. Before starting the synthesis, you may employ a base to precipitate them to the right metal hydroxides; however, this depends on the specific synthesis. The two most prevalent bases are sodium hydroxide and potassium hydroxide. This experiment makes use of ammonium hydroxide, a weak base. Nanostructures may be fine-tuned utilizing the hydrothermal method and a variety of surfactants, capping agents, and metal precursors. The wide variety of nanostructures produced by hydrothermal processing of metal oxides has the potential to improve a wide range of energy storage devices, including solar cells, sensors,

batteries, and supercapacitors.

The literature reports the synthesis of several CuO nanostructures using solution-based chemical methods. Copper precursor salts, soft template agents, and capping agents have all been investigated in various combinations. Copper salts such nitrate, chloride, sulphate, and acetate, together with HMTA, PEG+CTAB, Urea, HMTA+CTAB, SDBS, and PVP, have been the subject of several publications when combined with metallic Cu-powder. For the formation of different CuO nanostructures, such as 1-dimensional ones (nanowires, nano-ribons, nanorods), 2-dimensional ones (plate-like, leaflet-like, nanosheets), and 3-dimensional hierarchical ones (urchin-like, flower, carambola, oval, ellipsoid, spindle, and lenticular type), an additive and meticulous selection of Cu-precursor salts are necessary. The pH of the solution, the temperature, the concentration of the precursor, and the time of the deposition are all preparative factors that need further improvement. A higher surface-to-volume ratio and higher porosity may be achieved by modifying micro/nano structures, which in turn increases the number of sites favorable for fast reactions. The intra- and inter-granular/crystallite connections are much enhanced, which further facilitates charging. The electrolyte-solid interface, high electrical conductivity of the electrode material, high surface-to-volume ratio, and availability of active sites for bulk charge storage are the specific properties that make supercapacitors so effective. Specific capacitance increase, energy density, power density, electrochemical stability, and reversibility of supercapacitor materials are essential. Capping agents or surfactants allow for the customization of these properties.

When it comes to tailoring micro and nano structures, CTAB is a tried-and-true surfactant and additive. This ionic surfactant is adsorbed onto the surface of the crystallites in order to decrease the interfacial energy between them and the surrounding liquids. This makes it an ideal material for the electrode of a supercapacitor since it alters the pace and direction of crystallite development. The IUPAC name for CTAB is hexadecyl-trimethyl-ammonium bromide, and its chemical formula is [(C16H33)N(CH3)3]Br. A extensively used surfactant, CTAB is useful for regulating the nanoarchitecture during nanomaterial synthesis. The hydrothermal synthesis of CuO with the help of CTAB was described by Cao et al., who created a wide range of morphologies, including rod-like and hexahedron structures. The formation of CuO with a shuttle-like structure is achieved by the hydrothermal process of hydrolyzing cupric acetate at low temperatures using a CTAB. By experimenting with different surfactants and capping agents, the main objective of this study is to customize copper oxide nanostructures for usage in supercapacitors. By shortening the ion diffusion channel at the electrode-electrolyte interface, nanostructures improve supercapacitors by lowering diffusion resistance during ion transport.

Ammonium hydroxide, copper sulphate (CuSO4), and CTAB were among the analytical grade chemicals procured from Sigma Aldrich in India. No further purification is necessary before using these chemicals. The solutions have been made using water that has undergone two distillations. A range of copper sulfate solutions were prepared by dissolving the required amount of Cu precursor in double distilled water. This demonstrates the reduction action of ammonia, a weak base. You may make a weak base solution in water. Ammonia has a high solubility in water. Because of this, creating a solution of any concentration is a breeze. In this particular experiment, ammonia was used. The beaker already contains a solution of copper

sulfate and CTAB; the prepared solution is gradually added to it. Ammonium hydroxide is known to decrease a solution's turbidity. Once the addition is maintained at a certain level, the turbidity disappears completely. The stainless-steel substrate is carefully cleaned using zero-grit polish paper. To delicately tilt the cleaned substrate, the beaker is used. After that, everything is put in an autoclave and left alone to store. The autoclave is kept at a temperature of $90_{\beta}C$. For five minutes, the temperature remains at this level. It is then left to cool to room temperature. Once the substrate has reached room temperature, it is taken out of the autoclave.

To remove any contaminants from the steel substrate, we utilize water that has been double-distilled. After that, you need to give it a good air drying. N, cetyl trimethyl ammonium bromide is now mediating the deposition of black nanoparticles of copper oxide onto the substrate. Copper oxide nanoparticles may be synthesized by adjusting the proportion of copper sulfate. In this study, the amounts of copper sulfate varied between 0.1M and 0.5M. The CTAB concentration remained constant when the capping agent was used. New techniques of characterizing materials have the potential to provide insight on the shape, structure, and electrochemical behavior of nanoparticles. The nature and features of nanomaterials may be controlled by adjusting reaction parameters such as pH, temperature, reaction time, reducing agent type and amount, precursor and capping agent concentrations, and so on. In this study, we are focusing just on the precursor concentration and holding all other factors constant. Here is a rundown of some of the possible responses:

$$CuSO_4 + 2NH_3(aq) + 2H_2O \rightarrow Cu(OH)_2 + (NH_4)_2SO_4$$

Therefore, copper hydroxide is formed. Using an autoclave set to 90°C for 5 minutes, a nanostructured CuO thin film may be produced from Cu $(OH)_2$. It is feasible to find the reaction.

$$Cu(OH)_2 \xrightarrow{Hydrothermal\ at\ 90^{O}C\ for\ 5\ \text{min}} CuO + 2H_2O$$

Thin films of copper oxide were created by depositing a mixture of a constant concentration of CTAB in an aqueous solvent with precursors of varying concentrations of $CuSO_4$ (0.1-0.5M). The finished videos were considered for awards and $CuO_{0.1MCTAB}$, $CuO_{0.2MCTAB}$,$CuO_{0.3MCTAB}$,$CuO_{0.4MCTAB}$ and $CuO_{0.5MCTAB}$ respectively.

MATERIAL AND METHODS

Materials:

- Chemicals Used:
  - Copper sulfate (CuSO4): Used as the precursor.
  - Ammonium hydroxide: Used as the weak base.

- CTAB (cetyltrimethylammonium bromide): Used as a surfactant to limit the growth of copper oxide.
- All chemicals were of analytical grade and procured from Sigma Aldrich.
- Double-distilled water was used to prepare solutions.

Methods:

1. Preparation of Copper Oxide Thin Films:

- A range of copper sulfate concentrations (0.1M to 0.5M) were prepared by dissolving CuSO4 in double-distilled water.
- A constant amount of CTAB was added as a capping agent to the solution.
- Ammonium hydroxide was added gradually to the prepared solution to reduce turbidity.
- The solution was then poured onto a cleaned stainless-steel substrate, which was placed in an autoclave.
- The autoclave was kept at a temperature of 90°C for 5 minutes and then cooled to room temperature.

2. Film Formation and Characterization:

- Thin films of copper oxide were deposited on the substrate using the hydrothermal method.
- Characterization of the synthesized CuO thin films was performed using techniques such as:

- X-ray diffraction (XRD): To verify the crystallographic structure and phase of the CuO films.
- Scanning Electron Microscopy (SEM): To study the surface morphology.
- Brunauer-Emmett-Teller (BET) Method: Used to measure surface area and pore size distribution.
- Cyclic Voltammetry (CV): Used to evaluate the electrochemical performance of the CuO films.
- Galvanostatic Charge-Discharge (GCD): To determine the specific capacitance of the CuO films at different CuSO4 concentrations.

The study focused on understanding the influence of varying precursor concentrations of CuSO4 on the morphology and electrochemical properties of CuO thin films

Results And Discussion

XRD:

The use of XRD as a tool for structural and phase verification of CuO thin films supported by

CTAB is shown. The combination of XRD patterns of$CuO_{0.1CTAB}$,$CuO_{0.2CTAB}$to$CuO_{0.5CTAB}$in that order. The production of CuO is indicated by the strong and wide diffraction peaks of 2θ values of 35.5° and 38.35° in all XRD patterns, which correspond to the (-111), (111) planes. The diffraction peaks consistently showed that the CuO sample was in its monoclinic phase (ICDD card number 96-101-1149). We discovered that the produced material has a polycrystalline structure. The additional peaks, which correspond to the stainless-steel substrate, may be seen in the 2θ range of 42.5° to 80°. The marks Δ on the graph indicate these peaks. As the concentration of the CuS04 precursor solution increases, the XRD pattern shows that the crystallinity of the CuO nanoparticles improves. After eliminating the Cu Kα contribution and accounting for instrumental broadening in the pattern, the average crystallite size of the CuO was determined from the XRD pattern using the Scherer formula. In table 1, we can see the average size of the crystallites in CuO films made with different concentrations of CuSO4. The relationship between peak intensity and crystallite size grows linearly with increasing CuSO4 concentration. Concentrations over 0.4M, however, cause a drop in intensity. This suggests that the crystallinity grows with increasing CuSO4 concentration because there are more accessible solute centers to form the films. However, films deposited with a concentration over 0.4 M are further dissolved or etched, resulting in a drop in peak intensity.

CTAB-assisted CuO thin films were analyzed using X-ray diffraction to determine the crystallite nature and corresponding X-ray diffraction peaks with (hkl) Miller indices for CuO. These films were prepared using a variety of chemical techniques, including simple hydrothermal, wet chemical method, mild hydrothermal, facile hydrothermal, hydrothermal, and calcinations. The (-111, 111) axis is significant in all of these approaches, although additional maxima (110, (202), (202), (113), (-331), and (-220) are also documented.

Consistent with previously published values, our CTAB-assisted hydrothermally produced CuO on stainless steel substrate performed well. This research concludes that CuO does indeed exist in a monoclinic phase. The average size of the crystallites in our CTAB-assisted CuO samples is 16.38 nm, whereas the published value is 15 nm. The size of the crystallites in various CuO samples is shown in the table below.

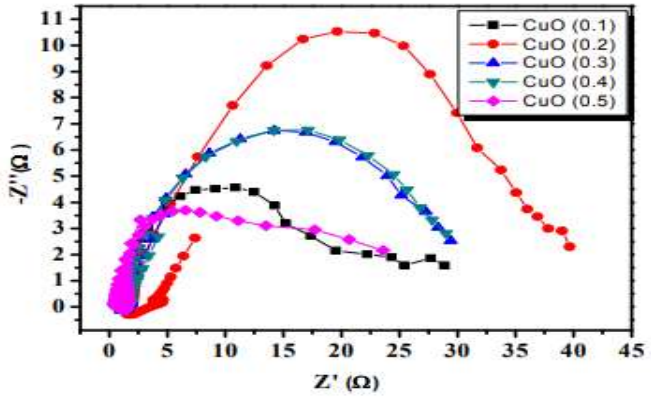

Fig 1: The XRD patterns of all the studied samples of CTAB assisted CuO thin films

Table No. 1: The summary of FWHM and crystallite size of CuO(0.1) to CuO (0.5) films.

$CuSO_4$con(M)	FWHM	Crystallite size(nm)
0.1	0.41	20.07
0.2	0.52	16.14
0.3	0.58	14.38
0.4	0.54	15.51
0.5	0.53	15.64

Scanning Electron Microscopy(SEM)

The thin films were examined using SEM to determine the impact of the capping agent (CTAB) on the morphology at various concentrations of $CuSO_4$. Surface morphology of the sample at various magnification scales is shown in Fig. 2 (a-e). This scanning electron micrograph looks like it may be a leaf. The homogeneous deposition of CuO nanostructure on stainless steel surfaces may be seen at reduced magnification. At concentrations of 0.4M and 0.5M, distinct morphologies and structures resembling leaves become apparent.

Growth Mechanism

Surfactant adsorption and desorption on CuO facets kinetically controls the growth rate in various directions as indexed by planes or faces. As part of the reaction process, CTAB breaks down into various spherical micelles, such as (CTA^+), which provide a coulombic force to$[Cu(OH)_4]^{2-}$causes reaction intermediates to be formed as (CTA^+ - $[Cu(OH)_4]^{2-}$). The development of CuO in certain directions, such (-111) and (111), is caused by this intermediate. The following response occurs:

$$NH_3.H_2O \rightarrow NH_4^+ + OH^-$$

$$Cu^{2+} + 2OH^- \rightarrow Cu(OH)_2$$

$$Cu(OH)_2 + 2OH^- \rightarrow [Cu(OH)_4]^{2-}$$

$$[Cu(OH)_4]^{2-} + (CTA^+) \rightarrow (CTA^+ - [Cu(OH)_4]^{2-}) \rightarrow CuO + H_2O + 2OH^-$$

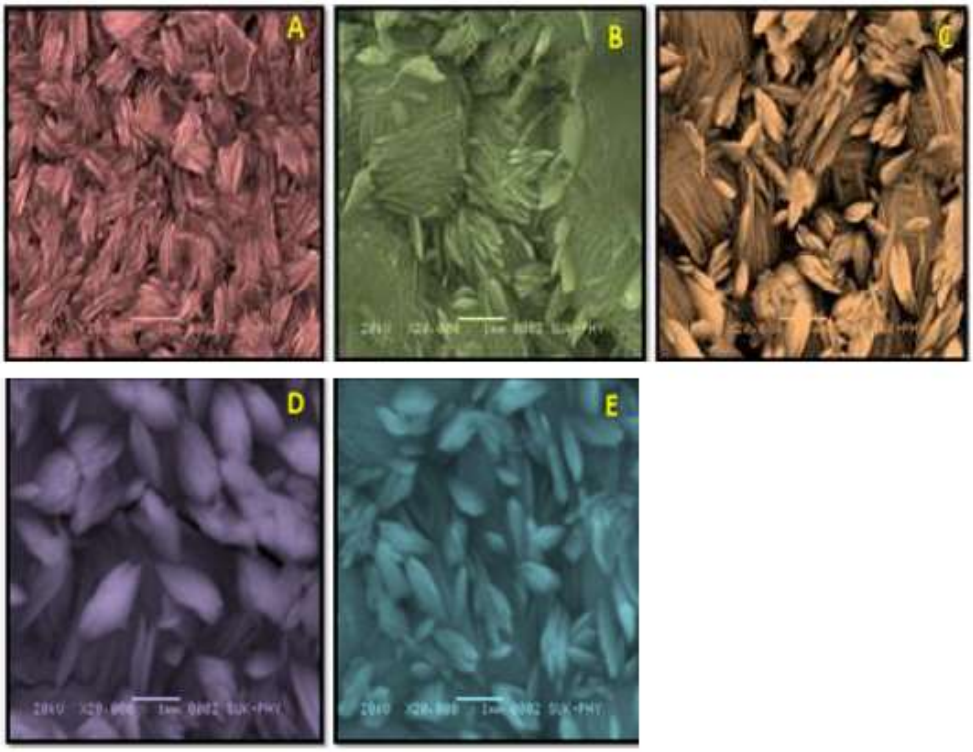

Fig 2: Scanning Electron Micrographs of the (a)$CuO_{0.1MCTAB}$ (b)$CuO_{0.2MCTAB}$ (c) $CuO_{0.3MCTAB}$ (d) $CuO_{0.4MCTAB}$ (e)CuO 0.5MCTAB samples at X 20,000 magnifications.

BET measurement

In order to determine the surface area and pore size distribution of the CuO films, the BET technique has been used to evaluate the physic-sorption of N2gas molecules on a solid surface. N2 adsorption and desorption isotherms were used to conduct BET measurements on CuO films ranging from 0.1 to 0.5. The results can be seen in Fig. 3(a-e), with the associated BJH pore size distribution plots shown in the inset graph. All CuO samples exhibited nitrogen isotherms of type IV, which is consistent with the existence of aggregated substrates resembling leaves. Table 2 shows the pore volume, BET specific surface area, and pore radius for all samples. The surfactant helped CuO understand that the surface area changed in response to changes in CuSO4 concentration. The graph below indicates that the surface area, pore radius, and pore volume of the CuO0.3CTAB sample are all rather big. Agglomeration of a capillary-like structure is seen when the CuSO4 concentration increases, leading to a reduction in surface area, pore radius, and pore volume. Structure and packing are correlated with the fluctuation of pore size distributions. Mesoporous yarn balls with capillary-like structures have a high specific surface area and pore volume/radius, making them useful for energy storage and increasing the number of places where chemical reactions may take place. Supercapacitor applications may be hindered by the limited charge storage capacity of CuO

electrodes caused by their compact nature, aggregation of leaf-like structures on microstructures, and tiny pore volume/radius.

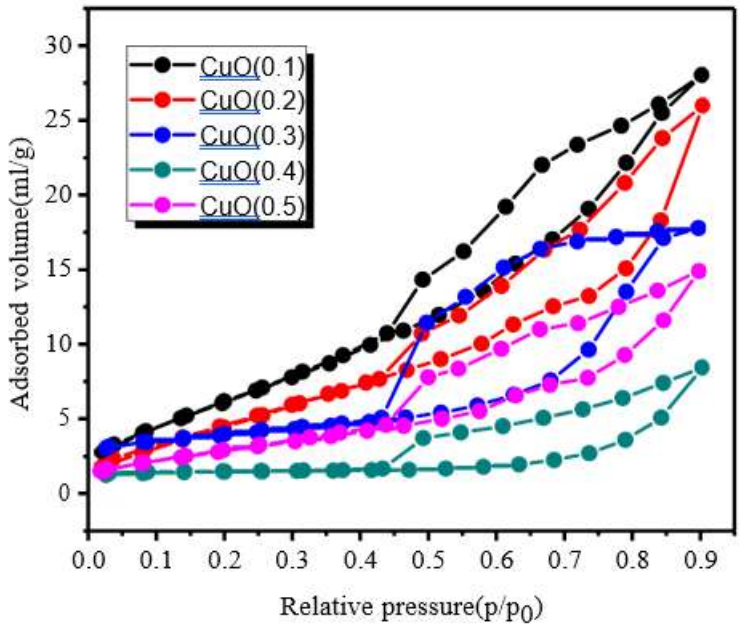

Fig 3 BET Graphs of all studied samples of CTAB assisted copper oxide thin films.

Table No.2: Surface area and poresize

$CuSO_4$Concentration	Poresize(nm)	Surfaceaream^2/g
0.1	4.19	36.03
0.2	4.95	29.65
0.3	4.37	34.57
0.4	6.36	12.30
0.5	4.67	20.53

Cyclic voltammetry

Cyclic voltammograms (CV) of all samples were recorded spanning -0.10V to 0.55 V vs. SCE at 10 mVs^{-1} in 1 M KOH to determine the oxidation and reduction potentials and the influence of the capping agent CTAB on $CuSO_4$ at varied concentrations on the electrochemical performance of CuO. An accompanying cathodic current occurs when the CuO sample is

scraped toward 0V vs. SCE $Cu^{2+} \rightarrow Cu^{1+}$ decrease procedure. In a similar vein, anodic current flows connected to $Cu^{1+} \rightarrow Cu^{2+}$ treatment by oxidation. The fact that electrodes may store charges is shown by the presence of cathodic and anodic peaks. The voltage difference between the cathodic and anodic peaks also increases the reversibility of the redox process. If cuprous oxide and/or cuprous hydroxide are oxidized to cupric oxide and/or cupric hydroxide, or if cupric oxide and/or cupric hydroxide are reduced to cuprous oxide and/or cuprous hydroxide, then the two peaks are widened here. Due to the complicated redox reaction of CuO in an alkaline solution, CV did not exhibit any additional noticeable peaks. The cellular redox process is shown by the following reaction: $Cu^{2+} + e^{-} \rightarrow Cu^{1+}$ A supersaturated condition is created when complex ions are formed, which inhibits spontaneous precipitation. Here is the formula to get CuO's specific capacitance.

$$Csp = \frac{\int Idv}{2m \times v \times dV}$$

where, Cspmaterial's specific capacitance, $\int Idv$ v scan rate, which is the integral area of the cyclic voltammetry curve, anddVpossible spectrum. According to this formula, the integral area of a cyclic voltammetry curve is exactly proportional to the specific capacitance of a material.

Here is a table that summarizes the computed SC values. The results show that the capacitances grow as the concentration goes from 0.1M to 0.2M. Capacitance remains unchanged when concentration is increased further. Based on these results, the ideal concentration for CuO films is 0.2M.

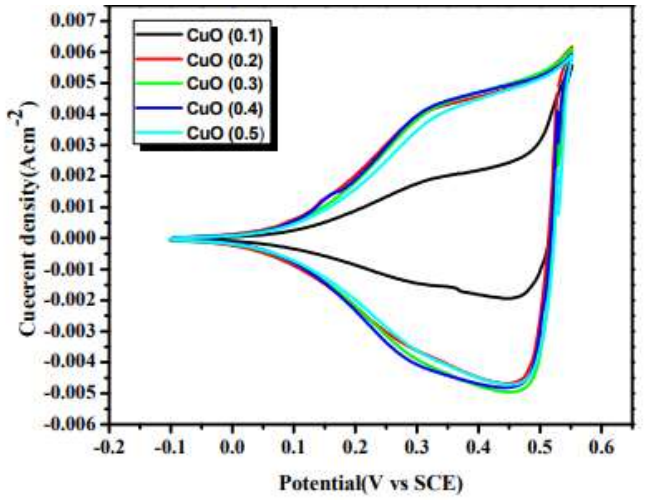

Fig 4: Cyclic Voltammograms of all the samples within a potential window of 0V to

0.55V

Galvanostatic charge discharge:

Galvanostatic charge/discharge graphs of all samples at 1 mA cm^{-2} in a potential range of 0 V to 0.55 V using an aqueous electrolyte of 1 M KOH are shown in Figure 5. This led researchers to conclude that the material exhibited optimal capacitive behavior with a nearly symmetric charge/discharge curve, since the curves were triangular in form. In addition, the minor non-linearity is indicative of a pseudocapacitive contribution, proving that this was the primary source of CuO's capacitance. This discharge curve primarily consists of three stages, including 1) the material's internal resistance as a result of the initial voltage drops. 2) The charge separation at the interface between the electrode and electrolyte causes the potential to vary linearly with respect to time, which in turn causes the double layer capacitance to arise. 3)The redox reaction between the electrolyte and electrode material was linked to the slope fluctuation of potential with time.

It is possible to calculate the specific capacitance as a function of $CuSO_4$ concentration using the galvanostatic discharge curves obtained from the following equation,

$$C_{sp} = \frac{Id \times Td}{M \times dv}$$

where$I_d$measures the density of applied current,$T_d$denotes the amount of active material, dv stands for the potential range, and M denotes the discharge duration.

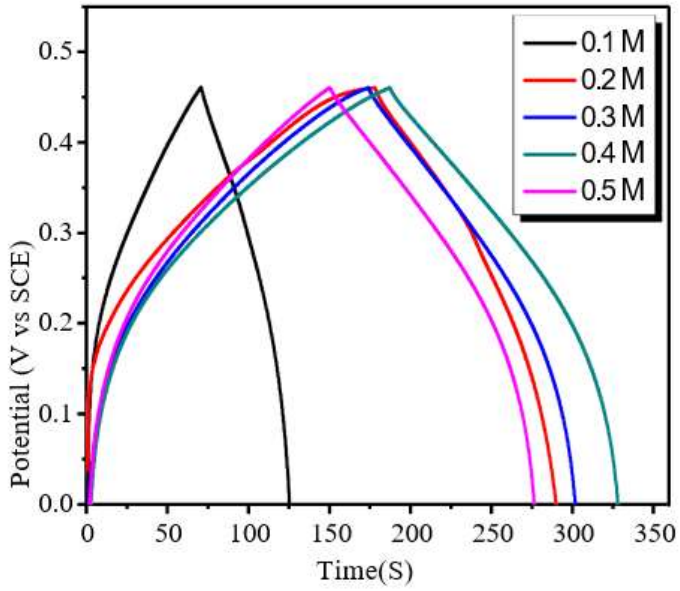

Fig 5: Galvanostatic Charge discharge curve of a11 the studied samples

Table No. 3: Specific capacitance values of CTAB assisted CuO for different concentrations

CTAB	CuO (M)	Deposited wt 10^{-4}gm	Absolute area 10^{-3} Cm^2	Specific Capacitance Fg^{-1}
5mM	0.1	9	1	45
5mM	0.2	22	3	52.5
5mM	0.3	37	3	88.1
5mM	0.4	35	3	82.5
5mM	0.5	31	3	78.2

CONCLUSIONS

A block co-polymer of poly ethylene and poly propylene covers the nanoparticles. Different concentrations of copper sulfate (0.1M, 0.2M, 0.3M, 0.4M, and 0.5M) are used to produce the nanoparticles in this case. Advanced characterization methods, including XRD and SEM, have been used to characterize the produced nanomaterials. The electrochemical performance behavior of the CTAB-assisted production of copper oxide nanoparticles shows that the optimal concentration is 0.5M of copper sulfate. Here, the hydrothermal technique is used to create Copper Sulfate in a variety of concentrations, including 0.1M, 0.2M, 0.3M, 0.4M, and 0.5M. Cetyltrimethylammonium ammonium bromide is the surfactant that is used. Every other variable, including pressure, temperature, capping agent, and precursor, remains constant. The only variable is the precursor concentration. At a concentration of 0.3M, the cyclic voltammetry results show a specific capacitance of 88.12Fg-1, which is the maximum value. At a scan rate of 10 mV/s and a capacitance retention of 80% after 1000 cycles. As a result, the surfactant-assisted CuO nanostructures fabricated using the simple and inexpensive hydrothermal approach exhibit outstanding electrochemical capacitive performance.

REFERENCES

1. Sumangala, T. & M. S., Sreekanth & Rahaman, Ariful. (2021). Applications of Supercapacitors. 10.1007/978-3-030-68364-1_11.
2. Yaseen, & Khattak, Muhammad & Humayun, Muhammad & Usman, Muhammad & Shah, Syed Shaheen & Bibi, Shaista & Bakhtiar, Syed Ul Hasnain & Ahmad, Shah & Khan, Abbas & Shah, Nasrullah & Tahir, Asif & Ullah, Habib. (2021). A Review of Supercapacitors: Materials Design, Modification, and Applications. Energies. 14. 7779. 10.3390/en14227779.
3. Prasad, G & Shetty, Nidheesh & Thakur, Simran & Rakshitha, & K. B., Bommegowda. (2019). Supercapacitor technology and its applications: a review. IOP Conference Series: Materials Science and Engineering. 561. 012105. 10.1088/1757-899X/561/1/012105.
4. Gao, Yuxiang. (2024). Research Status and Application of Supercapacitors. Highlights in Science, Engineering and Technology. 90. 105-111. 10.54097/gkstmy24.

5. Yadav, Sarita &Khone, Darshika & Ritu, & Rana, Abhimanyu Singh. (2024). Recent Developments in the Materials and Miniaturization of Supercapacitors. ChemNanoMat. 10.1002/cnma.202400011.
6. Oyedotun, Kabir & O. Ighalo, Joshua &Amaku, James &Olisah, Chijioke & Adeola, Adedapo &Iwuozor, Kingsley &Akpomie, Kovo& Conradie, Jeanet & Adegoke, Kayode Adesina. (2022). Advances in Supercapacitor Development: Materials, Processes, and Applications. Journal of Electronic Materials. 52. 10.1007/s11664-022-09987-9.
7. Minghai, Shen & Zhang, Yunyu& Ma, Hailing. (2021). Application and prospect of supercapacitors in Internet of Energy (IOE). The Journal of Energy Storage. 44. 103299. 10.1016/j.est.2021.103299.
8. Yılmazoğlu, Emre & Karakus, Selcan. (2023). Recent Developments in Nanostructured Materials for Supercapacitor Electrodes. Journal of the Turkish Chemical Society Section A: Chemistry. 10. 1107-1122. 10.18596/jotcsa.1320655.
9. Wahab, Y. & Naseer, Muhammad Nihal & Zaidi, Asad Ali & Umair, Talha & Khan, Hamdullah& Siddiqi, Muhammed Mobin & Javed, Muhammad Sabir. (2020). Super Capacitors in Various Dimensionalities: Applications and Recent Advancements. 10.1016/B978-0-12-819723-3.00020-2.
10. Libich, Jiri & Maca, Josef &Vondrák, Jiří & Cech, Ondrej &Sedlarikova, Marie. (2018). Supercapacitors: Properties and applications. Journal of Energy Storage. 17. 224-227. 10.1016/j.est.2018.03.012.
11. Rostami, Mohammad & Khodaei, Mohammad Mehdi. (2023). Recent advances of chitosan-based nanocomposites for supercapacitor applications: Key challenges and future research direction. The Journal of Energy Storage. 72. 10.1016/j.est.2023.108344.
12. Zhang, Lei & Hu, Xiaosong& Wang, Zhenpo& Sun, Fengchun& Dorrell, David. (2017). A Review of Supercapacitor Modeling, Estimation, and Applications: A Control/Management Perspective. Renewable & Sustainable Energy Reviews. 81. 10.1016/j.rser.2017.05.283.
13. Shah, Syed Shaheen & Aziz, Md. (2024). Properties of Electrode Materials and Electrolytes in Supercapacitor Technology. Journal of Chemistry and Environment. 3. 1–45. 10.56946/jce.v3i1.309.
14. He, Xiyue & Zhang, Xuelai. (2022). A comprehensive review of supercapacitors: Properties, electrodes, electrolytes and thermal management systems based on phase change materials. Journal of Energy Storage. 56. 106023. 10.1016/j.est.2022.106023.
15. Libich, Jiri &Sedlarikova, Marie & Maca, Josef &Čudek, Pavel &Fafilek, Guenter & Rodríguez, jaun& Prokes, Ales. (2023). Supercapacitors vs. Lithium-ion Batteries: Properties and Applications. ChemieIngenieur Technik. 96. 10.1002/cite.202300054.